Nanoscale ferroelectric switching behavior at charged domain boundaries studied by angle-resolved piezoresponse force microscopy

Moonkyu Park,[1] Seungbum Hong,[2,a)] Jiyoon Kim,[1] Jongin Hong,[3,a)] and Kwangsoo No[1,a)]
[1]*Department of Materials Science and Engineering, KAIST, Daejeon 305-701, Korea*
[2]*Materials Science Division, Argonne National Laboratory, Lemont, Illinois 60439, USA*
[3]*Department of Chemistry, Chung-Ang University, Seoul 156-756, Korea*

(Received 30 May 2011; accepted 7 September 2011; published online 7 October 2011)

We investigated the effect of charged domain boundaries (CDBs) on the coercive voltage (V_c) in polycrystalline $Pb(Zr_{0.25}Ti_{0.75})O_3$ (PZT) thin films using angle-resolved piezoresponse force microscopy (AR-PFM). By using the AR-PFM technique, we could observe the detailed domain structure with various degrees of CDBs including neutral domain boundaries in the PZT thin films. We found that the V_c increases at CDBs induced by polarization discontinuities. We attribute the change in V_c to the built-in field created by uncompensated polarization charges at the CDBs in the PZT thin films. © *2011 American Institute of Physics*. [doi:10.1063/1.3646761]

Ferroelectric materials have attracted widespread interest in various applications such as nonvolatile memories, RF identification tags, and energy harvesters.[1–3] When any system is miniaturized, the domain structure associated with ferroelectric properties becomes important. Thus, fundamental studies of domain structure and polarization switching phenomena at the nanometer scale are highly demanding.[4,5] Recently, piezoresponse force microscopy (PFM) has been used to characterize ferroelectric materials at the nanoscale via direct observation and modification of polarization states in ferroelectric domains.[6–9] Also, a combination of vertical and lateral PFM (VPFM and LPFM) has been used to reconstruct three-dimensional domain configurations in ferroelectric materials. Reconstruction of three-dimensional domain configurations enables us to investigate the domain boundaries and their effects on the electrical properties of ferroelectric materials. Rodriguez *et al.*[10] determined the three-dimensional polarization distribution in (111)-oriented PZT ferroelectric capacitors using VPFM data with two LPFM data sets and also studied charged domain boundaries (CDBs) in the capacitors related to imprint phenomena. Hong *et at.*,[11] reported the presence of CDBs contributed to leaky piezoresponse hysteresis loops in round-shaped $BiFeO_3$ nanostructures. Importantly, Seidel *et al.*,[12] observed the electronic transport properties dependence on the ferroelectric domain wall type in the $BiFeO_3$ thin films. More recently, Park *et al.*[13] suggested that angle-resolved piezoresponse force microscopy (AR-PFM) provides clearer information on the in-plane (IP) polarization direction and more direct observation of CDBs.

In spite of the extensive development of PFM techniques, the polarization behavior at surfaces and interfaces in polycrystalline thin films is not fully understood because of the presence of grains with different crystallographic orientation and various types of domain boundaries. Accordingly, it is crucial to visualize accurate ferroelectric domain structures in the polycrystalline films and understand the role of the CDBs in polarization switching and related phenomena. Herein, we image the map of polarization variants in polycrystalline $Pb(Zr_{0.25}Ti_{0.75})O_3$ (PZT) thin films using AR-PFM. This visualization allows an in-depth analysis of polarization charging at the domain boundaries on the piezoelectric properties.

We used 100 nm-thick polycrystalline PZT thin films deposited on Pt (150 nm)/SiO_2 (300 nm)/Si (100) substrates prepared by sol-gel deposition from INOSTEK Inc., Korea.[14] To better understand the nanoscale switching mechanism in polycrystalline PZT thin films, it is essential to reconstruct three-dimensional domain configurations at the sub-grain level. Previously, we verified that the combination of the IP-PFM phase contrast and sample rotation angle (θ) more accurately resolved IP domain polarization directions than using both IP-PFM amplitude and phase contrasts (AR-PFM).[13] Figure 1(a) shows a map of all possible IP polarization directions overlaid with grain boundaries. Individual color regions in the map represent specific IP polarization directions, and the color corresponds to the orientation of ferroelectric domains. Each color is also assigned a specific number in the coordination. Out-of-plane (OP) PFM amplitude and phase signals of the same region are shown in Figs. 1(b) and 1(c), respectively. The OP-PFM phase image showed bright contrast over the entire scan area, whilst OP PFM amplitude signals were inhomogeneous, indicative of random crystallographic orientation.[15]

To gain insights into polarization charging at domain boundaries and their effect on ferroelectric switching behavior, we used Eq. (1) to calculate the polarization charges per unit area at the boundaries. We can find the amount of polarization charges per unit area at the segment where the two polarization variants meet at the boundary using

$$\sigma_p = \sum P_i \cdot n_i = P_2 \cdot \cos\theta_2 - P_1 \cdot \cos\theta_1, \qquad (1)$$

where σ_P is the interface charge per unit area arising from the discontinuity of P along the interface normal vector, P_i is the polarization of domain i, and θ_i is the angle between P_i and the surface normal vector of the interface. The underlying assumptions are (a) IP polarization is a unit vector

a)Authors to whom correspondence should be addressed. Electronic addresses: hong@anl.gov, hongj@cau.ac.kr, and ksno@kaist.ac.kr.

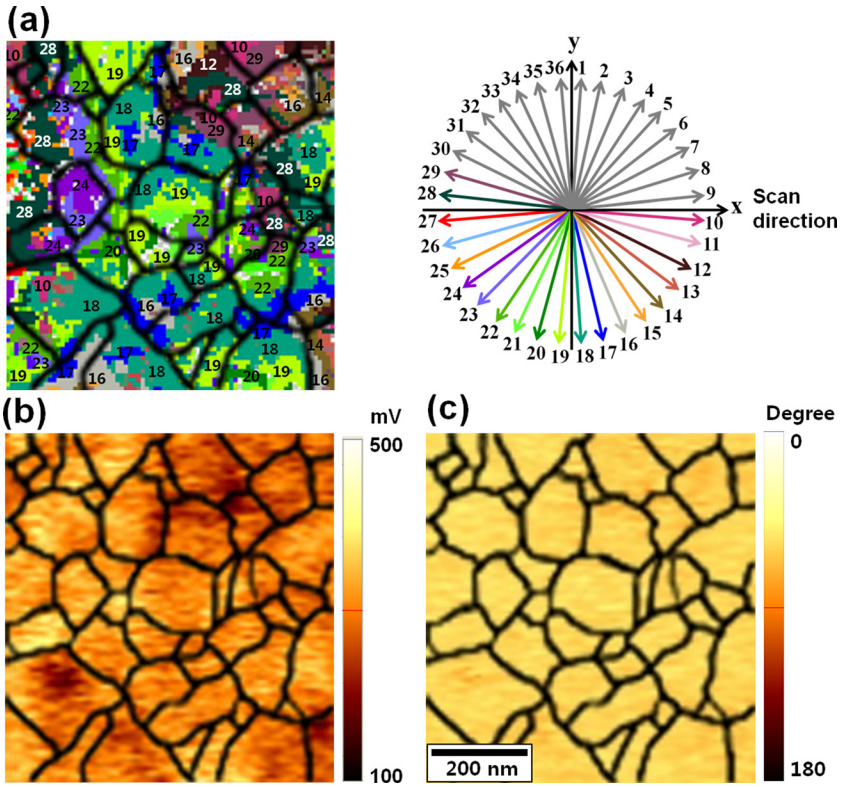

FIG. 1. (Color online) (a) A map of all possible IP polarization directions constructed by AR-PFM. (b) OP-PFM amplitude, and (c) phase images of vertically poled PZT thin film.

($P_1 = P_2$) and (b) a segment where two polarization variants meet in the domain boundary is a line and normal to the surface. Figure 2 illustrates all possible polarization configurations for neutral and charged domain boundaries. Figs. 2(a) and 2(b) show the schematics of neutral domain boundaries (NDBs) and CDBs, respectively. Figs. 2(a1) and 2(a2) show anti-parallel polarizations and discontinuous polarizations with the same absolute θ_i values whereas Figs. 2(b1), 2(b2), and 2(b3) show discontinuous polarizations with different θ_i values, *head-to-head* and *tail-to-tail* configurations, respectively. We note that, in our experimental results, we observed all the possible polarization configurations except the anti-parallel polarizations. The *head-to-head* (or *tail-to-tail*) IP polarization configuration results in the maximum accumulation of positive (or negative) charges at the domain boundary. Although the CDB between *head-to-head* or *tail-to-tail* polarization regions carries a large electrostatic energy penalty, this may be due to the competing interactions of the strain field in the poled sample or growth kinetics of film nuclei, as described in our previous work.[10,13]

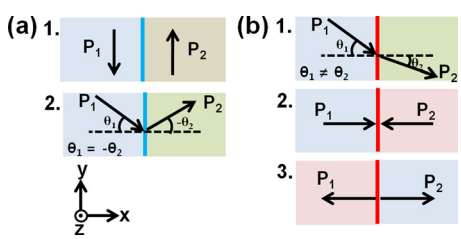

FIG. 2. (Color online) Possible polarization configurations: (a) NDBs ((1): anti-parallel polarizations and (2): discontinuous polarizations with the same absolute θ_i values), (b) CDBs ((1): discontinuous polarizations with the different θ_i values, (2): *head-to-head*, and (3): *tail-to-tail* configurations. Black arrows, light gray (blue) lines, and dark gray (red) lines represent the polarization directions, NDBs and CDBs, respectively.

Although all kinds of CDBs were present in the films, we found that most of the CDBs contained polarization charge less than 0.5 P in its absolute amount (where P is the surface charge density of remnant polarization). This might show a prevalence of mildly charged domain boundaries characterized by the *head-to-tail* IP configuration depicted in Fig. 3(b). To correlate the extent of polarization charging at those CDBs with the positive coercive voltage (V_c^+) of piezoresponse hysteresis loops, we collected the hysteresis loops from 10 regions in the PZT thin films.[14] We used only V_c^+ for the analysis since the initial state of domain configuration is changed after the first switching with positive voltages (first half of the loop) of the hysteresis loop measurement. We acquired an average of five values at each voltage step. We found that the standard deviation of V_c^+ of the loops at the NDBs was 0.6 V. This standard deviation is proportional to the contribution of the factors other than polarization charging that could be considered noise. Therefore, we used 0.6 V as a criterion to evaluate the influence of polarization charging on the hysteresis loops. We believe that this fluctuation might be caused by a built-in field at the interface of the bottom electrode/ferroelectric thin film and work function difference dependence on grain orientation.[7,16]

As there could be many factors influencing the shift of the loops, we averaged the hysteresis loops collected from various regions with similar degrees of polarization charging. We observed that the averaged hysteresis loop measured at CDBs had higher coercive voltage (3.19 ± 0.53 V) than that taken from the NDBs (1.98 ± 0.61 V), i.e., inside of single domains (Figure 3(a)). In addition, the mild charging of negative polarization resulted in higher V_c^+ than NDBs. This can be understood with the schematics shown in Fig. 3(b), where we show the mild CDB created by discontinuous polarization configurations. In Fig. 3(b), the negative

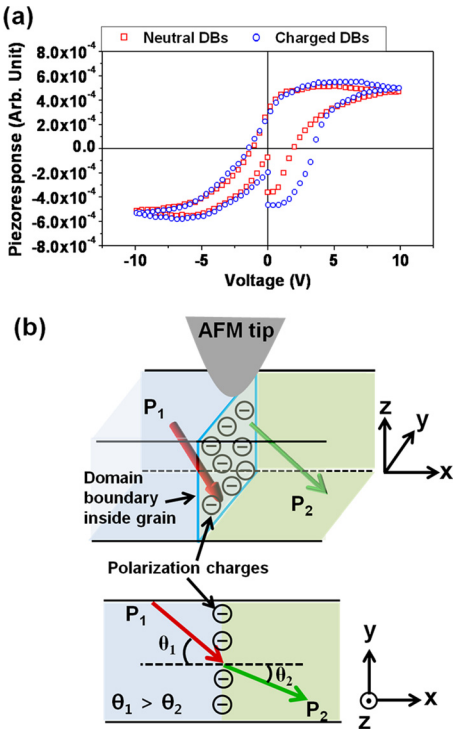

FIG. 3. (Color online) (a) Piezoresponse hysteresis loops from NDBs and CDBs and (b) schematics of domain configuration and charge distribution at the charged domain boundary. Dashed lines represent surface normal lines of domain boundaries.

polarization charging is expected at the CDB because θ_1 is larger than θ_2. This raises the built-in field at the CDB to increase the V_c^+ obtained at the CDB. This result supports the fact that the CDBs can be the dominant source of change in V_c in polycrystalline ferroelectric films, which may lead to the imprint phenomena.

Notably, the local hysteresis loops (in Figs. 3(a)) showed discontinuity at the initial and ending points. We believe that the abnormal hysteresis loop was caused by the surface charges on the PZT films injected from the conductive tip during the poling process. Electric charges can contribute to the PFM signal as explained by Hong *et al.*[17] We believe that first measured hysteresis loops showed discontinuity due to the electrostatic effect by the injected surface charges. The electrostatic effect was drastically reduced during dc voltage sweep for hysteresis loop measurements for the first measurement due to the charge relaxation as explained by Kim *et al.*[18,19] They reported that the surface charges are deposited on the PZT thin films to screen the polarization charges during the poling process. They also observed the lower surface charge distribution at the grain boundary than inside the grain. In addition, we found that the difference between initial and ending point of the hysteresis loop was larger in the hysteresis loops obtained inside grains than that obtained at the grain boundaries (the difference between initial and ending points of the hysteresis loops obtained inside grains and at the grain boundaries were $2.774 \times 10^{-4} \pm 1.442 \times 10^{-4}$ and $1.814 \times 10^{-4} \pm 1.063 \times 10^{-4}$ in the arbitrary unit, respectively) which supports the validity of our hypothesis.[14]

In conclusion, we have visualized IP polarization variants in the vertically poled polycrystalline PZT thin films using AR-PFM. We have discussed all the possible configurations for both CDBs and NDBs in PZT films. Most of the CDBs were mildly charged, which had a significant effect on the coercive voltage of piezoresponse hysteresis loops.

This research was supported by the Nano R&D Program (No. 2010-0019123), Basic Science Research Program (No. 314-2008-1-D00172), Conversion Research Center Program (No. 2011K000674), and Mid-career Researcher Program (No. 2010-0015063) through the National Research Foundation (NRF) funded by the Ministry of Education, Science and Technology (MEST), New & Renewable Energy of the Korea Institute of Energy Technology Evaluation and Planning (KETEP) grant funded by the Ministry of Knowledge Economy, Republic of Korea (No. 20103020060010). Work at Argonne National Laboratory (S.H., design of experiments, data analysis, and writing of manuscript) was supported by UChicago Argonne, a U.S. DOE Office of Science Laboratory, operated under Contract No. DE-AC02-06CH11357. J.H. acknowledges a start-up fund supported by Chung-Ang University.

[1]H. Ko, K. Ryu, H. Park, C. Park, D. Jeon, Y. K. Kim, J. Jung, D.-K. Min, Y. Kim, H. N. Lee, Y. Park, H. Shin, and S. Hong, Nano Lett. **11**, 1428 (2011).
[2]N. Setter, D. Damjanovic, L. Eng, G. Fox, S. Gevorgian, S. Hong, A. Kingon, H. Kohlstedt, N. Y. Park, G. B. Stephenson, I. Stolitchnov, A. K. Taganstev, D. V. Taylor, T. Yamada, and S. Streiffer, J. Appl. Phys. **100**, 051606 (2006).
[3]M. Kim, M. Hoegen, J. Dugundji, and B. L. Wardle, Smart Mater. Struct. **19**, 045023 (2010).
[4]A. Gruverman and A. Kholkin, Rep. Prog. Phys. **69**, 2443 (2006).
[5]S. V. Kalinin, A. N. Morozovska, L. Q. Chen, and B. J. Rodriguez, Rep. Prog. Phys. **73**, 056502 (2010).
[6]S. Hong, J. Woo, H. Shin, J. U. Jeon, Y. E. Pak, E. L. Colla, N. Setter, E. Kim, and K. No, J. Appl. Phys. **89**, 1377 (2001).
[7]A. Gruverman, A. Kholkin, A. Kingon, and H. Tokumoto, Appl. Phys. Lett. **78**, 2751 (2001).
[8]V. Nagarajan, S. Aggarwal, A. Gruverman, R. Ramesh, and R. Waser, Appl. Phys. Lett. **86**, 262910 (2005).
[9]S. V. Kalinin, B. J. Rodriguez, S. Jesse, E. Karapetian, B. Mirman, E. A. Eliseev, and A. N. Morozovska, Annu. Rev. Mater. Res. **37**, 189 (2007).
[10]B. J. Rodriguez, A. Gruverman, A. I. Kingon, R. J. Nemanich, and J. S. Cross, J. Appl. Phys. **95**, 1958 (2004).
[11]S. Hong, J. A. Klug, M. Park, A. Imre, M. J. Bedzyk, K. No, A. Petford-Long, and O. Auciello, J. Appl. Phys. **105**, 061619 (2009).
[12]J. Seidel, L. W. Martin, Q. He, Q. Zhan, Y.-H. Chu, A. Rother, M. E. Hawkridge, P. Maksymovych, P. Yu, M. Gajek, N. Balke, S. V. Kalinin, S. Gemming, F. Wang, G. Catalan, J. F. Scott, N. A. Spaldin, J. Orenstein, and R. Ramesh, Nature Mater. **8**, 229 (2009).
[13]M. Park, S. Hong, J. A. Klug, M. J. Bedzyk, O. Auciello, K. No, and A. Petford-Long, Appl. Phys. Lett. **97**, 112907 (2010).
[14]See supplementary material at http://dx.doi.org/10.1063/1.3646761 for sample information, detailed experimental conditions of PFM measurements and measured hysteresis loops.
[15]C. Harnagea, A. Pignolet, M. Alexe, and D. Hesse, Integr. Ferroelectr. **44**, 113 (2002).
[16]L. F. Zagonel, M. Bäurer, A. Bailly, O. Renault, M. Hoffmann, S.-J. Shih, D. Cockayne, and N. Barrett, J. Phys.: Condens. Matter **21**, 314013 (2009).
[17]J. W. Hong, K. H. Noh, S. Park, S. I. Kwun, and Z. G. Khim, Phys. Rev. B **58**, 5078 (1998).
[18]Y. Kim, M. Park, S. Bühlmann, S. Hong, Y. K. Kim, H. Ko, J. Kim, and K. No, J. Appl. Phys. **107**, 054103 (2010).
[19]Y. Kim, S. Bühlmann, J. Kim, M. Park, K. No, Y. K. Kim, and S. Hong, Appl. Phys. Lett. **91**, 052906 (2007).